

# MIT/LL development of broadband linear frequency chirp for high-resolution ladar

Kevin W. Holman, David G. Kocher, Sumanth Kaushik

Lincoln Laboratory, Massachusetts Institute of Technology  
244 Wood St., Lexington, MA 02420-9108

## ABSTRACT

The development of a high-resolution laser radar (ladar) exhibiting sub-mm resolution would have a great impact on standoff identification applications. It would provide biometric identification capabilities such as three-dimensional facial recognition, interrogation of skin pore patterns and skin texture, and iris recognition. The most significant technical challenge to developing such a ladar is to produce the appropriate optical waveform with high fidelity. One implementation of such a system requires a 1.5-THz linear frequency sweep in 75  $\mu$ s. Previous demonstrations of imaging with such waveforms achieved a 1 THz sweep in  $> 100$  ms, and required additional corrections to compensate for sweep nonlinearity. The generation of high fidelity, temporally short frequency-swept waveforms is of considerable interest to the DoD community. We are developing a technique that utilizes a novel method to generate a 1 THz sweep in 50  $\mu$ s from a mode-locked laser. As a proof-of-principle demonstration of this technique we have successfully generated a 20 GHz sweep in 1  $\mu$ s with a fidelity sufficient to produce better than -20 dB sidelobes for a range measurement without using any additional corrections. This method is scalable to produce the entire 1 THz sweep in 50  $\mu$ s.

**Keywords:** laser radar; ladar; lidar; arbitrary waveform generation; linear frequency modulation; chirp; mode-locked laser

## 1. INTRODUCTION

Existing state-of-the-art laser radar (ladar) systems offer a resolution of a few centimeters, which provides the ability to resolve and identify large objects such as vehicles. However, a high-resolution ladar would enable precise identification of personnel from standoff distances. A resolution of 1 cm would enable the determination of a person's gait, which could have some limited identification value. 1-mm resolution would enable three-dimensional facial recognition that is not dependent on the head position or lighting. Once systems move to higher resolutions it becomes possible to resolve finer structural details, such as skin pore patterns and textures ( $\sim 0.1$  mm) and stromal features in the iris ( $\sim 50$   $\mu$ m). Iris recognition is attractive for its high specificity and low false alarms. Ultrahigh resolution systems that enable sub-mm resolution will rely on the precise generation of unique optical waveforms. We have developed a technique that will enable the generation of such a waveform, and we have completed initial proof-of-principle demonstrations of this technique.

## 2. REQUIREMENTS FOR HIGH-RESOLUTION LADAR

In a 3-D ladar, range measurements are provided by measuring the round trip time of transmitted pulses that are scattered by the object of interest. A high range resolution requires this time to be measured with sufficient precision. In a direct-detection ladar, this time-of-flight measurement is limited by the length of the transmitted pulses and the timing resolution of the detector. Although mode-locked lasers exist that provide pulses with durations of only a few fs, which would yield a range resolution of  $< 1$   $\mu$ m, current detector technology does not enable the timing resolution sufficient to resolve these short pulses. This would require a detector with an electronic bandwidth in excess 150 THz. However, a coherent technique that has been used in radar systems can be adapted to the optical regime to avoid

detector limitations.<sup>1</sup> This technique is referred to as stretch processing, where a temporally long pulse is transmitted, and upon receiving, pulse compression algorithms are used to reduce the effective length of the pulse and improve the effective resolution. A suitable waveform to use for this technique is a linear frequency ramp, as shown in Fig. 1. The bandwidth of the frequency chirp ( $B$ ) determines the range resolution of the system, independent of the chirp time ( $T$ ), which is chosen to accommodate properties of the target and detector. The time-delayed returned waveform (dashed blue line in Fig. 1) is combined onto a photodetector with a copy of the transmitted signal (red solid line) to produce the heterodyne beat frequency between the two optical signals. This heterodyne beat frequency is directly proportional to the target range. It is important to keep the phase and amplitude noise of the waveform as small as possible to reduce the sidelobe level of the beat frequency. This is crucial for distinguishing multiple scattering points on the target. The advantage of this coherent technique is that the bandwidth requirements of the detector are significantly reduced, while a high resolution is still achievable. The total optical bandwidth  $B$  determines the resolution, while the detector bandwidth requirement is given by the maximum beat frequency  $F$ , and thus the dynamic range of the system.

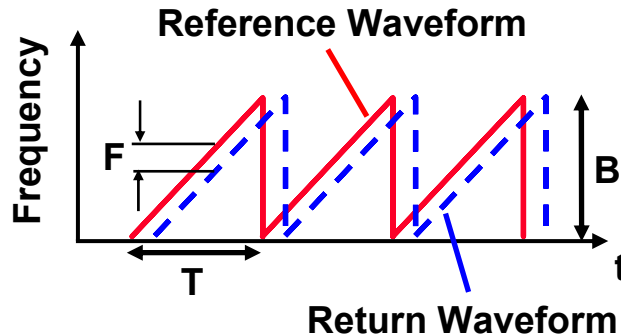


Fig. 1. Linear frequency modulated waveform. Heterodyne beat frequency provides range information.

For imaging applications, the lateral resolution should be comparable to the range resolution. However, a 100- $\mu\text{m}$  resolution at a standoff range of a few hundred meters would require a prohibitively large aperture due to diffraction effects. Therefore, the lateral resolution is improved using synthetic aperture processing. When the target moves laterally with respect to the lidar system, reconstruction of the phase history of the heterodyne signal allows the creation of a synthetic aperture that is much larger than the physical aperture of the system.<sup>2</sup> This can be viewed as using the Doppler shift due to the target's motion to determine the relative radial velocity between the source and target scattering point, and thus the angle to the scatterer. Since only one sample of the heterodyne signal phase is acquired during each chirp time,  $T$ , this time must be sufficiently short to allow a sufficiently high sample rate to satisfy the Nyquist condition for sampling the Doppler bandwidth of the target as it passes by the source. In a typical encounter, the Doppler bandwidth is expected to be  $\sim 13$  kHz, requiring a chirp time of 75  $\mu\text{s}$  (each chirp provides one complex sample). To achieve a 100- $\mu\text{m}$  resolution, a chirp of 1.5 THz is required, and thus a chirp rate of 50  $\mu\text{s} / \text{THz}$ . One notable aspect of synthetic aperture processing is that it provides a resolution that is independent of the range.

### 3. GENERATION OF BROADBAND FREQUENCY SWEEP

There have been other recent efforts to develop high-resolution lidar systems that utilize linear frequency chirps.<sup>3,4</sup> These efforts have produced some nice results, but they have been limited by the ability to produce a high bandwidth chirp in a short time. They have relied on frequency sweeping of tunable external cavity diode lasers, producing sweep rates of 1 THz in 0.8 s<sup>3</sup> and 1 THz in 0.1 s<sup>4</sup>. Also, because of nonlinearities of the chirp, the work in Ref. 3 required the use of a reference path matched to the target distance. This is obviously not suitable for use outside of the laboratory, where the target distance is not known a priori. In Ref. 4 post-processing techniques removed the need for a matched reference delay. However, it is desirable to eliminate the phase noise of the generated waveform, and to produce much faster chirps to accommodate large Doppler bandwidths for synthetic aperture processing. The generation of phase-controlled trains of wide-band, temporally short chirped pulses is of considerable interest to the DoD community.<sup>5</sup>

The novel chirp generation technique we have devised will enable the production of a 1 THz chirp in 50  $\mu\text{s}$ . It is summarized in Fig. 2. A broadband 1.5- $\mu\text{m}$  mode-locked laser is used as the source. However, instead of using the

short pulses produced by the mode-locked laser, the regularly spaced discrete frequencies it provides are used as the building blocks of a linear frequency chirp. This comb of frequencies spans the entire spectral range of the desired chirp, and through external manipulation of the frequency components a linear frequency sweep is generated. First, the comb is separated to transmit each frequency component along a separate optical fiber. The comb spacing is determined by the laser repetition frequency, which is 10 GHz. The fabrication of arrayed waveguide devices with a channel spacing of 10 GHz has been reported,<sup>6</sup> which would be suitable for this demux operation. Each frequency then passes through an electro-optic intensity modulator, which passes each frequency for 0.5  $\mu$ s, and then extinguishes that frequency for the remainder of the chirp time. The timing of the modulators is adjusted so that recombination of the frequencies produces a stair-step waveform of frequency vs. time. An adjustable delay line immediately after the modulators allows phase control of the frequencies for compensating any relative drifts of the path lengths, as described in Section 3.2. The stair-step waveform is then transmitted through an optical single sideband generator<sup>7</sup> that is driven with an RF chirped waveform. The RF waveform produces a chirp from 5 – 15 GHz in 0.5  $\mu$ s. This introduces a sideband on the optical frequencies (the transmitted carrier is nulled) that sweeps 10 GHz, and matches up with the beginning of the sweep of the next optical frequency's sideband. The subchirps are phase coherently stitched together (described in Section 3.2) using the phase control mentioned earlier to produce a total chirp of  $N \times 10$ GHz in  $N \times 0.5\mu$ s, where  $N$  is the number of frequency channels. The two significant challenges of implementing this scheme are the generation of the 10 GHz RF chirp in 0.5  $\mu$ s, and the phase coherent stitching of multiple subchirps. These topics are covered in the next two sections.

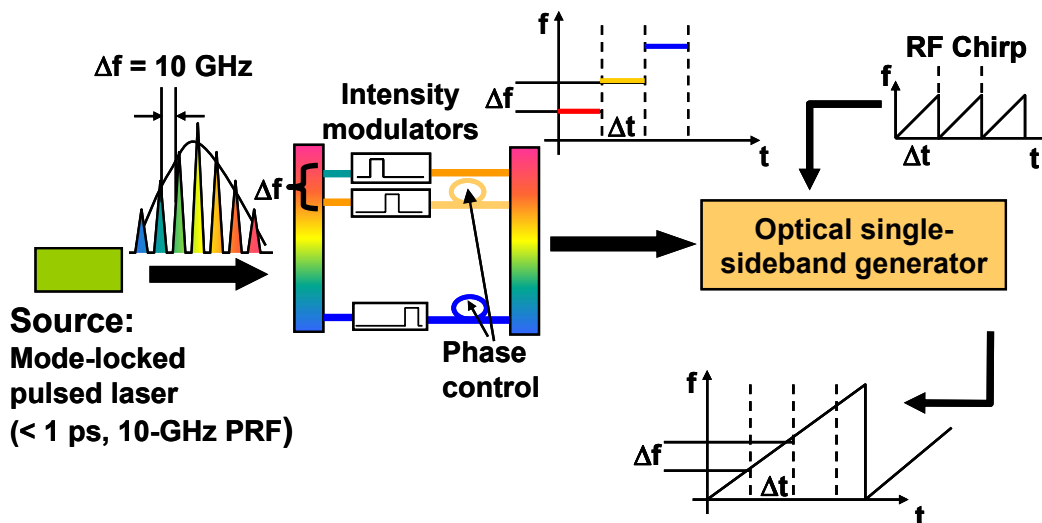


Fig. 2. Generation of broadband linear frequency chirp from mode-locked laser source. Each of the frequency components are chirped 10 GHz with a single-sideband modulator. These subchirps are then phase coherently combined to form the complete chirped waveform.

### 3.1 RF waveform generation

Since the chirped optical waveform is essentially made up of copies of the RF chirped waveform shifted up to optical frequencies, the quality of the final optical waveform is dependent on the RF waveform to have low phase and amplitude noise. The RF chirp is generated digitally, and is produced as shown in Fig. 3. A 2-channel digital arbitrary waveform generator is used, which provides a 1.25 GS/s sample rate, and an analog bandwidth of 500 MHz. The two channels drive the I and Q inputs of an RF single-sideband generator, producing a signal that sweeps from 4 GHz - 500 MHz to 4 GHz + 500 MHz. This 1 GHz chirped signal then passes through 4 stages of frequency doublers, multiplying the chirp bandwidth to 16 GHz, with a 64 GHz center frequency. Mixing down with a 54 GHz signal provides a RF signal from 2 – 18 GHz. Though the system has the capability to provide a 16 GHz chirp, only 10 GHz is needed, and the waveform produced by the digital arbitrary waveform generator is adjusted accordingly.

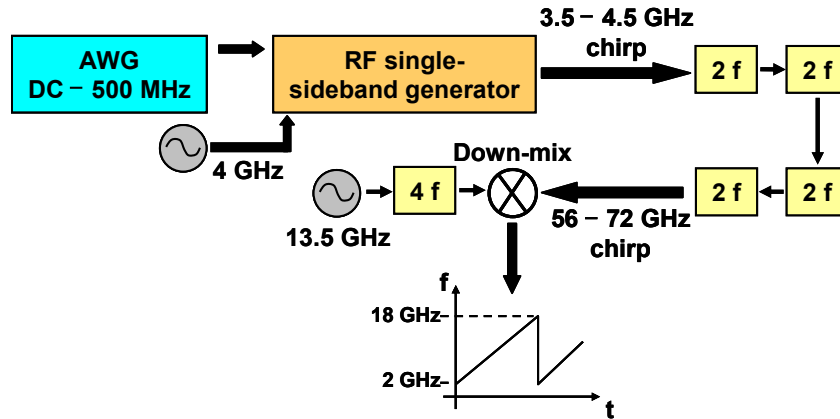


Fig. 3. Digital generation of RF chirped waveform. Arbitrary waveform generator (AWG) drives single-sideband generator to produce 1 GHz chirp. 16x frequency multiplication provides 16 GHz chirp capability.

The generation of a highly linear RF chirp with low amplitude and phase distortion requires compensation for the distortions introduced by the frequency doublers and other microwave components prior to the optical single sideband generator. This is accomplished by measuring the phase of the RF chirp in a delayed heterodyne setup and appropriately adjusting the amplitude and phase of the I and Q inputs to the RF single sideband generator. The quality of the chirp is characterized by splitting the chirped signal, transmitting one portion through a delay line, and mixing the chirped signal with the delayed copy on a power detector. This simulates the return from a point target, and the Fourier transform provides the point spread function (PSF) of the generated signal. Low sidelobes are necessary to distinguish multiple scattering centers in a distributed target. An analogous setup is used to characterize the optical chirp once the RF chirp is used to drive the optical single sideband modulator. Figure 4 shows the PSF for the 10-GHz RF and optical chirps, with delays of 9 ns and 10 ns, respectively. There is no degradation of the optical PSF as compared to the RF result, indicating that the RF signal is reliably imposed onto the optical frequency and that the sidelobe level is limited by the quality of the RF chirp. A sidelobe level of  $< -20$  dB is achieved for chirping a single optical frequency.

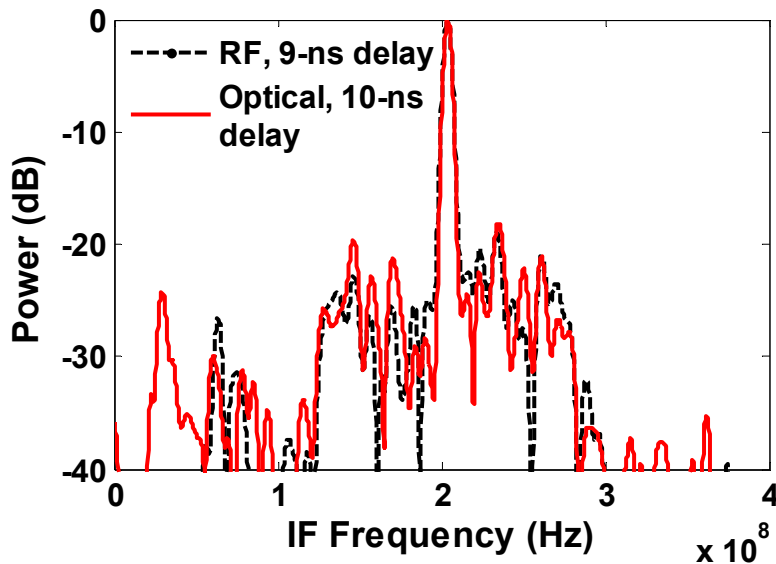


Fig. 4. PSF for RF and optical chirps. Measured with delayed heterodyne technique. Performance limited by RF chirp.

### 3.2 Phase-coherent combination of multiple subchirps

With the demonstration of a 10-GHz RF chirp and the ability to reliably transfer this to an optical frequency, the remaining challenge is to phase-coherently stitch together several 10-GHz optical chirps to piece together a continuous wide-band chirp. Since a mode-locked laser serves as the source of the optical frequencies, there is already very little high-frequency relative phase noise among the frequency components. The dominant source of relative noise is due to differential path length fluctuations during the time when each frequency is traveling on separate optical fibers. The delay lines in each path are used to eliminate this relative fluctuation, and to set the phase of each frequency to provide a continuous chirped signal.

We have completed a proof-of-principle demonstration of our technique for stitching together multiple subchirps to produce a broadband phase-coherent chirp. We have combined two subchirps to produce a 20-GHz chirp. The setup to detect the phase noise between two frequency components and produce a 2-subchirp total chirp is summarized in Fig. 5a. Since the electro-optic modulators are never transmitting at the same time, it is not possible to directly beat the transmitted optical frequencies on a detector to measure their relative phase fluctuations. However, by rotating the polarization of the light before entering the electro-optic modulators, it is possible to take advantage of the strong dependence of the extinction ratio on the polarization of the light. This dependence is shown in Fig. 5b. By operating between the two points denoted by the black lines ( $< 8$  V and  $< 12$  V), the light polarized along the slow-axis of the PM fiber in the system will experience 27 dB attenuation, while the fast-axis light will experience only 0.5 dB attenuation. After recombining the two optical frequencies, a polarizing beamsplitter is used to separate the fast-axis and slow-axis polarizations. The slow-axis light yields the stair-step waveform shown in Fig. 2, which subsequently passes to the optical single sideband generator for chirping. The fast-axis light is directed to a photodetector, which produces the 10-GHz beat signal between the two frequencies. The relative phase fluctuations are determined by mixing this signal with a stable 10-GHz reference, which is phase-coherent with the repetition frequency of the mode-locked laser. The phase fluctuations are then eliminated by feeding back to the adjustable delay line in one of the optical paths.

The stabilization scheme described above successfully removes any high-frequency fluctuations up to several kHz. However, due to slowly changing birefringence in the optical fiber, there is a slow drift in the relative phase for the slow-axis light vs. the stabilized fast-axis light. This occurs on a timescale of approximately a minute. This is mitigated by monitoring the beat signal between the chirped optical waveform and a delayed copy of itself. An example of such a waveform is shown in Fig. 5c for a 1-GHz RF chirp, with an optical frequency spacing of only 1 GHz. There is an overlap region, denoted by the dashed lines, where the end of the first optical chirp beats with the beginning of the second optical chirp. This is the only region where the phase of the RF beat signal depends on the relative phase of the two optical frequencies, since when the first chirp is beating with itself, and the second chirp is beating with itself, any common phase offset cancels. Monitoring the phase of this overlap region allows the DC value of the locked phase to be adjusted to eliminate any phase discontinuity at the beginning and end of the overlap region, as has been done to produce the data in Fig. 5c. This adjustment is performed by adjusting the phase of the 10-GHz reference to which the 2-line beat signal is stabilized. There remains a slow drift in the relative amplitudes of the individual subchirps due to this slowly changing birefringence, and techniques to eliminate this are currently under investigation.

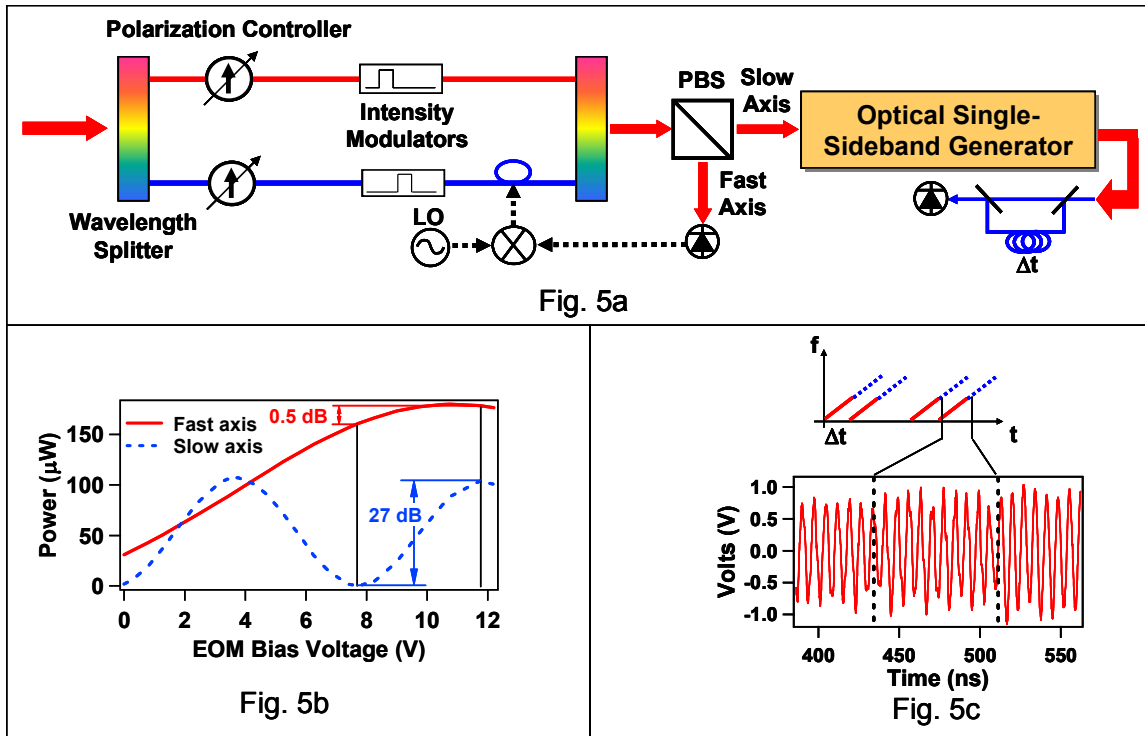


Fig. 5. (a) Setup for detecting and canceling relative phase fluctuations of two optical frequency components. (b) Polarization dependence of electro-optic intensity modulators. (c) Heterodyne signal before, during, and after inter-chirp overlap for self-delayed beat measurement.

Figure 6 shows the PSF of the optical waveform for combining two 10-GHz chirps to produce a full 20-GHz chirp in 1  $\mu\text{s}$ . These data were obtained by beating the chirped waveform with itself, with a relative delay of 71 ns. Figure 6a reveals the importance of matching the bandwidth of the chirp to the optical frequency spacing. We found that the corrections applied to the RF chirp to compensate for the aberrations of the frequency doublers and other microwave components had altered the chirp bandwidth from the intended value by 6 MHz. This mismatch causes a phase discontinuity in the RF heterodyne signal between the portion where the first chirp is beating with itself and the portion where the second chirp is beating with itself, which is independent of the phase between the two optical frequencies. This phase discontinuity causes the splitting of the central peak seen in Fig. 6a. To correct this condition the optical frequency spacing was adjusted, although it could not be set exactly equal to the chirp bandwidth because the product of the chirp time and the optical frequency spacing must be an integer to maintain the phase of the heterodyne signal in the overlap region from chirp to chirp. This can be understood by considering that the difference in the phase accumulations of the two optical frequencies from one chirp to the next must be an integer multiple of  $2\pi$ . With the optical frequency spacing set as close as possible to the RF chirp bandwidth while satisfying this time-bandwidth condition, the PSF shown in Fig. 6b was achieved. The blue trace shows the high sidelobes present when the relative phase of the two optical frequencies is set incorrectly. Proper adjustment of this stabilized phase produces the red trace, with sidelobes  $< -20$  dB. Fig. 6c compares the PSF for the combined 20-GHz chirp with that obtained from a single chirp of 10 GHz. Because of the increased measurement time, the linewidth of the central lobe is reduced from 3 MHz to 1.3 MHz. Given the sweep rate of 20 GHz /  $\mu\text{s}$ , this corresponds to an improvement in the range resolution from 2 cm to 1 cm.

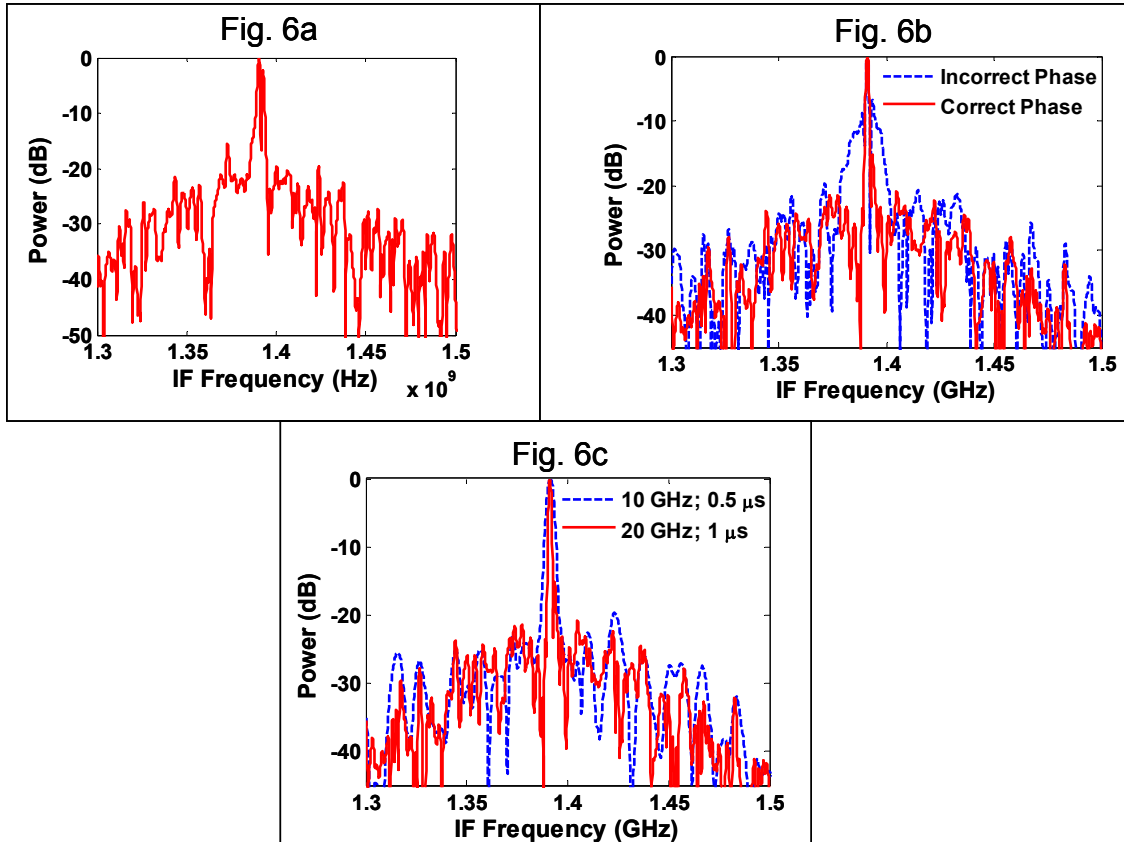


Fig. 6. (a) PSF for 20-GHz optical chirp, with mismatch between RF chirp bandwidth and optical frequency spacing. (b) PSF of 20-GHz chirp for adjusted and incorrect relative phase of optical frequencies. (c) Comparison of PSF of 10-GHz and 20-GHz optical chirps.

#### 4. SUMMARY

We have devised a method to generate a wide-band linear frequency chirp from the discrete frequency components of a mode-locked laser. This is of interest for developing ultrahigh resolution lidar systems that will enable standoff biometric imaging. Our method for chirp generation involves external manipulation of the laser output to produce a stair-step pattern of frequency vs. time. A single sideband generator is then used to chirp each ‘step’ up to the next ‘step.’ Phase control of the individual frequency components allows the phase-coherent stitching of these individual subchirps to produce a continuous wide-band linear frequency chirp. So far we have successfully demonstrated the generation of the 10-GHz chirped RF waveform that yields -20 dB sidelobes. This waveform has successfully been imposed onto an optical frequency, and we have demonstrated the ability to phase-coherently combine two subchirps to produce a 20-GHz chirp in 1  $\mu$ s.

The current sidelobe level is limited by the RF chirp, and the chirp bandwidth is still not exactly equal to the optical frequency spacing due to the compensation of phase aberrations of the microwave components. This is causing the remaining ‘knee’ on the high-frequency side of the central lobe in Figs. 6b and 6c. Future work will include efforts to further improve the phase correction of the RF chirp. In addition, investigations are underway to eliminate the slow amplitude drifts caused by birefringence in the phase-stitching setup, as mentioned in Section 3.2. Incorporation of more frequency channels will provide a proportionally better resolution. The current polarization scheme for detecting relative phase noise is not appropriate for scaling beyond two frequency components, and we are investigating variations on this technique that will enable phase corrections when more frequency channels are implemented.

## ACKNOWLEDGEMENTS

The authors thank R. M. Heinrichs for valuable discussions, and J. H. Kyung and L. Jiang for their contributions in the early stages of this work. This work is sponsored by the United States Air Force under AF Contract #FA8721-05-C-0002. Opinions, interpretations, recommendations and conclusions are those of the authors and are not necessarily endorsed by the United States Government.

## REFERENCES

- 1.) W. J. Caputi, *IEEE Trans. Aero. Electr. Syst.*, AES-7 (1971).
- 2.) J. C. Curlander and R. N. McDonough, *Synthetic Aperture Radar: Systems and Signal Processing* (Wiley, New York, 1991).
- 3.) M. Bashkansky, R. L. Lucke, E. Funk, L. J. Rickard, and J. Reintjes, *Opt. Lett.* **27**, 1983 (2002).
- 4.) W. Buell, N. Marechal, J. Buck, R. Dickinson, D. Kozlowski, T. Wright, and S. Beck, *Laser Radar Tech. and Apps. X*, G. W. Kamerman ed. (SPIE, Bellingham, WA, 2005), Vol. 5791 of Proc. of SPIE, 152.
- 5.) DARPA DSO Ultra-broadband Optical Arbitrary Waveform Generation Program, BAA 05-11.
- 6.) K. Takada, M. Abe, T. Shibata, and K. Okamoto, *IEEE Photon. Tech. Lett.* **13**, 577 (2001).
- 7.) S. Shimotsu, S. Oikawa, T. Saitou, N. Mitsugi, K. Kubodera, T. Kawanishi, M. Izutsu, *IEEE Photon. Tech. Lett.* **13**, 364 (2001).